

# Patterns of U-Pb zircon and monazite ages in polymetamorphic units of the Swiss Central Alps

Autor(en): **Köppel, V. / Günthert, A. / Grünenfelder, M.**

Objektyp: **Article**

Zeitschrift: **Schweizerische mineralogische und petrographische Mitteilungen  
= Bulletin suisse de minéralogie et pétrographie**

Band (Jahr): **61 (1981)**

Heft 1

PDF erstellt am: **21.07.2024**

Persistenter Link: <https://doi.org/10.5169/seals-47132>

## **Nutzungsbedingungen**

Die ETH-Bibliothek ist Anbieterin der digitalisierten Zeitschriften. Sie besitzt keine Urheberrechte an den Inhalten der Zeitschriften. Die Rechte liegen in der Regel bei den Herausgebern.

Die auf der Plattform e-periodica veröffentlichten Dokumente stehen für nicht-kommerzielle Zwecke in Lehre und Forschung sowie für die private Nutzung frei zur Verfügung. Einzelne Dateien oder Ausdrucke aus diesem Angebot können zusammen mit diesen Nutzungsbedingungen und den korrekten Herkunftsbezeichnungen weitergegeben werden.

Das Veröffentlichen von Bildern in Print- und Online-Publikationen ist nur mit vorheriger Genehmigung der Rechteinhaber erlaubt. Die systematische Speicherung von Teilen des elektronischen Angebots auf anderen Servern bedarf ebenfalls des schriftlichen Einverständnisses der Rechteinhaber.

## **Haftungsausschluss**

Alle Angaben erfolgen ohne Gewähr für Vollständigkeit oder Richtigkeit. Es wird keine Haftung übernommen für Schäden durch die Verwendung von Informationen aus diesem Online-Angebot oder durch das Fehlen von Informationen. Dies gilt auch für Inhalte Dritter, die über dieses Angebot zugänglich sind.

## **Patterns of U-Pb zircon and monazite ages in polymetamorphic units of the Swiss Central Alps**

by *V. Köppel\**, *A. Günthert\*\** and *M. Grünenfelder\**

### **Abstract**

The Lepontine area of the Swiss Central Alps underwent during the Alpine orogeny an amphibolite facies metamorphism. The U-Pb age patterns of zircons from meta-igneous rocks and metasediments are very similar to those from areas not affected by this mid-Tertiary tectono-thermal event.

From the zircon data which also include zircon suites of pebbles and matrix of presumably pre-Permian metaconglomerates, it is concluded that the pre-Mesozoic rocks comprise:

- metasediments deposited probably during the late pre-Cambrian to Cambrian,
- approximately 450 m. y. old granitic rocks,
- middle Palaeozoic metasediments, and
- approximately 300 m. y. old granitic rocks which form the bulk of the pre-Mesozoic rocks in the Lepontine area.

Zircon age patterns of granitic gneisses exhibit a regional trend. In the Simplon-Antigorio area, zircons contain no or only small amounts of older components. The upper intercept ages cluster around 300 m. y. To the east, populations with varying but generally distinct amounts of inherited components dominate, indicating that these granitic rocks are mainly of sedimentary anatexis origin.

The formation of migmatites occurred approximately 280 m. y. ago according to monazite ages. In spite of the thermal metamorphism during the Alpine orogeny these monazite ages are only 10 to 30% discordant, thereby demonstrating the resistivity of the U-Pb system in monazites to such events. Young concordant monazite ages of about 23 m. y. indicate the end of the amphibolite facies metamorphism in the central part of the Lepontine area.

### **Introduction**

The nappes of the Lepontine gneiss region comprise the deepest tectonic units of the Penninic realm. They consist mainly of granitic gneisses, i. e. K-feldspar-plagioclase-biotite-muscovite gneisses of granitic to granodioritic, less fre-

---

\* Swiss Federal Institute of Technology - Zurich

Laboratory for Isotope Geology and Massspectrometry Sonneggstrasse 5, CH-8092 Zürich

\*\* Mineralogisch-Petrographisches Institut der Universität, Bernoullistrasse 30, CH-4056 Basel

quently quartzmonzonitic composition. Metasediments form the second most important group; they are represented by plagioclase-biotite-muscovite gneisses and schists. Amphibolites are rare.

Mesozoic sediments separate the different nappe units. To the North, Jurassic to Cretaceous schists separate the Penninic zone from the parautochthonous Gotthard massive (fig. 1). Southwards the Mesozoic sediments form comparatively thin bands of marbles, dolomites and calcisilicate rocks. To the South, the Lepontine area is separated from the Southern Alps by the Insubric line.

The northward thrustured nappes were updomed in the Leventina and the Verampio area (at sample locality 8, fig. 1). Between these two culminations, a synform structure (Maggia Querzone) runs approximately N-S and swings to the East as it approaches the root zone in the South.

During the Tertiary Alpine orogeny the complex was metamorphosed under amphibolite facies conditions. Remnants of an early Alpine, or older, high-pressure metamorphism are recognized in tectonic fragments of ultramafic rocks which occur as boudins, often associated with carbonate and calcisilicate rocks, within the Simano nappe or possibly between the Simano and Adula nappes (EVANS and TROMMSDORFF, 1978, FREY et al., 1980). For a comprehensive discussion of the Alpine metamorphism, the reader is referred to the paper by FREY et al. (1974).

One of the major questions concerns the age of the granitic gneisses and the migmatites within the Lepontine area. The possibility that these gneisses represent early Alpine intrusions was supported by the presence of pegmatites along the root zone (WENK, 1969) and of postkinematic intrusions of granodioritic rocks in the Bergell area (GULSON and KROGH, 1973). Textural and mineralogical evidence indicates that all gneisses recrystallized under amphibolite facies conditions and were affected by the same deformations during the Alpine orog-

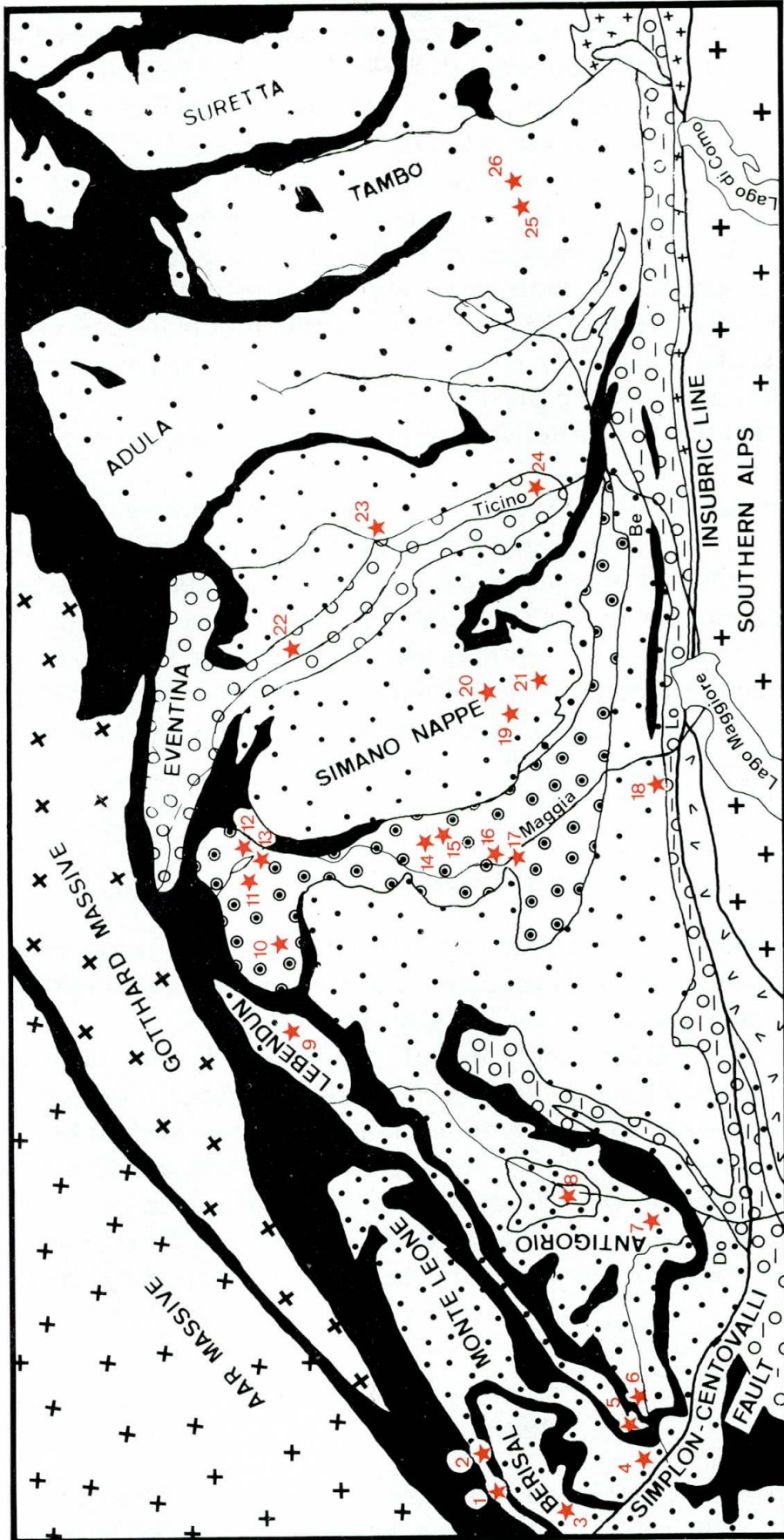
Fig. 1 Samples

|               |                  |          |           |                |          |
|---------------|------------------|----------|-----------|----------------|----------|
| 1 EIS         | (Eisten) *       | Z (1)    | 17 GIUM 1 | (Giumaglio) ** | M        |
| 2 GAT         | (Ganter) *       | Z (2)    | 17 GIUM 2 | (Giumaglio) ** | M, Z (2) |
| 3 BES         | (Berisal) *      | Z (2)    | 18 TEG    | (Tegna) *      | Z (1)    |
| 4 MLE         | (Monte Leone) *  | Z (1)    | 19 BRI 1  | (Brione) *     | Z (2)    |
| 5 LEB 1       | (Lebendun) *     | Z (1)    | 20 BRI 2  | (Brione) **    | M        |
| 6 ANT 1       | (Antigorio) *    | Z (1,2)  | 21 BRI 4  | (Brione) **    | M        |
| 7 ANT 2       | (Antigorio) *    | Z (1)    | 22 LEV 1  | (Leventina) *  | Z (2,1)  |
| 8 VER         | (Verampio) *     | Z (1)    | 23 SIM    | (Simano) *     | Z (2)    |
| 9 LEB 2       | (Lebendun) **    | Z (3,2)  | 24 LEV 2  | (Leventina) *  | Z (2)    |
| 10 BRA 1      | (P. di Braga) ** | Z (2)    | 25 RH 816 | (Bodengo) ***  | Z (2)    |
| 10 BRA 2      | (P. di Braga) ** | Z (2)    | 26 RH 814 | (Bodengo) ***  | Z (2)    |
| 11 MATO 1     | (Matorello) **   | Z (2)    | 26 RH 824 | (Bodengo) ***  | Z (2)    |
| 12 MATO 2     | (L. Sambocco) ** | Z (3)    |           |                |          |
| 13 FUSIO **   |                  | M        |           |                |          |
| 14 RUSCADA ** |                  | M, Z (2) |           |                |          |
| 15 COCCO **   |                  | M, Z (2) |           |                |          |
| 16 SOMEO **   |                  | M        |           |                |          |

M: Monazite; Z: Zircon (number refers to group 1-3, Figs. 2 + 3)

\* C.J. ALLÈGRE et al., 1974; \*\* this paper;

\*\*\* R. HÄNNY et al., 1975



Scale  
20 kilometres

Fig. 1

Penninic units :

- Leventina gneiss
- ◌ Bosco-series, zones of Locarno, Bellinzona and Orselina
- ⊙ Maggia Querzone
- Mesozoic metasediments and greenstones (penninic and helvetic)
- ⊠ (other) Penninic nappes

- Lo: Locarno
- Be: Bellinzona
- Do: Domodossola

- ⊠ Crystalline rocks of massives and Southern Alps
- ⊕ Tertiary intrusions
- ⊖ Sesia-zone (lower austro-alpine unit)

eny. Nowhere were intrusive contacts observed between granitic gneisses and Mesozoic metasediments; their occurrence is restricted to pre-Mesozoic rocks. Likewise, migmatization is only observed in pre-Mesozoic rocks (WENK, 1969).

The aim of the investigation was hence to establish with the aid of U-Pb zircon ages of different grain size fractions and varying magnetic susceptibilities (for references see GEBAUER and GRÜNENFELDER 1979) whether the granitic gneisses represent early Alpine intrusives or else were formed during Palaeozoic or even earlier magmatic-metamorphic events. The investigation was carried out over a period of more than 10 years. Some of the results have already been published (ALLÈGRE et al., 1974). HÄNNY et al. (1975) analyzed migmatites in the Bodengo Valley and on the basis of U-Pb zircon and Rb-Sr whole rock data demonstrated that the migmatites were of pre-Alpine, i.e. Palaeozoic, origin.

The investigation was pursued to include zircons from metasediments. GÜNTHERT et al. (1976) reported a case of an isochemical granitization of psammitic and psephitic rocks within the Maggia nappe. Zircon analyses from such rocks, including a boulder sized pebble, were performed in order to test the granitization hypothesis put forward by these authors and also in the hope of obtaining age brackets for the sedimentation of the psephitic gneisses. In addition a migmatite outcrop in the Maggia valley offered a further opportunity to analyze a case of a possible Alpine migmatization.

#### Analytical Procedure

The previously reported zircon data were obtained by the borax fusion method and by extracting lead with dithizone and uranium with aluminumnitrate and hexone or with anion exchange resin in nitrate form.

The results reported in Tables 2 and 3, except sample Mato 1, were obtained by the method developed by KROGH (1971). Minor modifications are: the zircon concentrates were crushed in an agate mortar and one part was used for determining the isotopic composition of lead and the other part was spiked with a combined  $^{208}\text{Pb}$ - $^{235}\text{U}$  solution prior to dissolution. Prior to extraction of the lead used for the isotope composition the resin was washed with 2N HCl in order to minimize the lead loss. The monazite chemistry is reported by CORFU (1980).

#### Results

The results are listed in Table 2 and 3, and the data points are plotted in figures 2 and 3. A  $^{238}\text{U}/^{206}\text{Pb}$  versus  $^{207}\text{Pb}/^{206}\text{Pb}$  diagram was chosen because, in

Table 1 Reproducibility of U/Pb ratio of sample ANT 1 30–42  $\mu\text{m}$ , n. m.

| ppm U | rad.<br>ppm Pb | U/Pb  |
|-------|----------------|-------|
| 935   | 32.96          | 28.37 |
| 919   | 32.43          | 28.35 |
| 922   | 32.50          | 28.36 |
| 913.5 | 32.30          | 28.28 |

contrast to the conventional  $^{206}\text{Pb}/^{238}\text{U}$  vs.  $^{207}\text{Pb}/^{235}\text{U}$  diagram, the pronounced curvature of the concordia curve allows a better visual examination of the data pattern.

The uncertainty of the  $^{238}\text{U}/^{206}\text{Pb}$  ratio was estimated from the reproducibility (table 1) to be  $\pm 0.5\%$ . The uncertainty of the corrected  $^{207}\text{Pb}/^{206}\text{Pb}$  ratio was derived by considering the standard deviations of the measured  $^{207}\text{Pb}/^{206}\text{Pb}$  and  $^{206}\text{Pb}/^{204}\text{Pb}$  ratios and the extreme values of the corrected  $^{207}\text{Pb}/^{206}\text{Pb}$  ratio when using a common lead with ratios:  $^{206}\text{Pb}/^{204}\text{Pb} = 18.30$  and  $^{207}\text{Pb}/^{204}\text{Pb}$  varying from 15.25 to 15.75. The  $^{207}\text{Pb}/^{204}\text{Pb}$  ratio of 15.5 for the common lead correction was chosen as a compromise between a measured blank composition ( $^{207}\text{Pb}/^{204}\text{Pb} \sim 15.4$ ) and lead from Palaeozoic galena ore of the Alps ( $^{207}\text{Pb}/^{204}\text{Pb} = 15.60$  to  $15.68$ ). In contrast to the  $^{207}\text{Pb}/^{206}\text{Pb}$  and  $^{207}\text{Pb}/^{235}\text{U}$  ages the  $^{206}\text{Pb}/^{238}\text{U}$  age is quite insensitive to the choice of the  $^{206}\text{Pb}/^{204}\text{Pb}$  correction.

It should be noted that the analytical errors of the previously published results (compare list of figure caption 1) are considerably bigger than those reported in table 2. The less sophisticated method of data acquisition, the comparatively poor reproducibility of the isotopic composition analyses due to the previously used sample loading technique and the lack of absolute isotope standards introduced additional uncertainties. Therefore the apparent scatter of data points of a zircon suite is probably not significant (fig. 3). All zircon suites, except BRA 2, shown in fig. 3 form linear arrays within analytical uncertainties.

#### THE MONAZITE U-Pb AGE

From table 3 and fig. 3 it is evident that two age groups exist, one with apparent ages of 21 to 23 m.y. and a second one with apparent U-Pb ages of 200 to 300 m.y. Ages of the younger group are reproducible to within  $\pm 0.5$  m.y., the older within  $\pm 5$  m.y. The question arises whether the young ages are truly concordant or not, i.e. yielding identical  $^{206}\text{Pb}/^{238}\text{U}$  and  $^{207}\text{Pb}/^{235}\text{U}$  ages. Analytical errors and the uncertainty of the common lead correction normally do not allow to recognize whether this condition is fulfilled or not. For such young ages the  $^{207}\text{Pb}/^{206}\text{Pb}$  age is very sensitive to small changes of the ratio; a change

of 0.5% results in a change of the age by 12 m.y. Further complications may arise from radioactive disequilibria at the time of crystallization. Variations of the initial  $^{234}\text{U}/^{235}\text{U}$  ratio of  $\pm 10\%$ , however, do not seriously affect ages of 20 m.y. or higher (LUDWIG, 1977).

On a  $^{207}\text{Pb}/^{204}\text{Pb}$ - $^{206}\text{Pb}/^{204}\text{Pb}$  plot the data points form a linear array with a slope of  $0.04682 \pm 0.00060$  corresponding to a  $^{207}\text{Pb}/^{206}\text{Pb}$  age of  $40 \pm 30$  m.y. ( $2\sigma$  errors); thus this age is within the error identical to the U-Pb ages and therefore compatible with the assumption of concordancy. The  $^{207}\text{Pb}/^{206}\text{Pb}$  age is, however, high when compared to the U/Pb ages. The best fit line, which goes through all data points within their analytical errors except one sample, passes well below any reasonable common lead, e.g.  $^{206}\text{Pb}/^{204}\text{Pb} = 18.50$ ,  $^{207}\text{Pb}/^{204}\text{Pb} = 15.29$ . Recalculating the line with a hypothetical common lead point at  $^{206}\text{Pb}/^{204}\text{Pb} = 18.50$  and  $^{207}\text{Pb}/^{204}\text{Pb} = 15.65$ , which closely approximates K-feldspar lead isotopic compositions from the Lepontine region, yields a slope of  $0.04626 \pm 0.00025$  corresponding to an age of  $11 \pm 13$  m.y. These results show that the monazites are free of inherited lead, in contrast to zircons from magmatic rocks.

Further support for the concordancy of the young monazite ages is found in the observation that different size fractions yield identical ages within analytical uncertainties (KÖPPEL et al., in preparation). At the present, we can therefore assume that the young monazite ages of about 20 m.y. are concordant.

The monazite samples which yielded apparent ages between 200 and 300 m.y. were observed in the upper central part of the Maggia valley region along the western flank of the Maggia Querzone. From table 2 and figure 3 it can be seen that, in contrast to the first group, these ages are discordant and that the degree of discordance is related to the grain size. The nature of the discordancy is, however, not clear. The U-Pb system of the monazites may well have been partially open during the Alpine metamorphism, or else the samples consist of two generations of monazites, an Alpine and a Hercynian one. The two samples from granitic gneisses (GIUM 2, COCCO) exhibit a similar age pattern with an upper intercept on the concordia curve at 270 to 285 m.y. The sample from the paragneiss GIUM 1 has a higher upper intercept age of 285 to 305 m.y. The pattern of the data points is remarkable insofar as the tie-lines between the two fractions of each of the samples has a positive slope. However, the uncertainties of the  $^{207}\text{Pb}/^{206}\text{Pb}$  also permit the construction of tie-lines with negative slopes and the maximum lower intercepts with the concordia curve are 65 m.y. for sample GIUM 2, 38 m.y. for GIUM 1 and 15 m.y. for COCCO.

The existence of old monazites in an area where this mineral normally yields young concordant ages indicates that the young monazites were newly formed during the Alpine metamorphism. According to OVERSTREET (1967) the occurrence of monazite in metamorphic rocks of greenschist to lower amphibolite facies is rare due to the instability of the mineral under such conditions. The dis-

tribution of monazite in the Lepontine area agrees with these findings; monazite is rare in the western part whereas in the eastern part where upper amphibolite facies conditions were reached during the Alpine metamorphism it is frequently encountered as a minor rock forming constituent.

## ZIRCONS

Fig. 2 and 3 show the data points of all zircon suites from the Lepontine area west of the Mera Valley including those already published (ALLÈGRE et al.,

Table 2 Analytical data of zircon samples

| SAMPLE<br>size fraction<br>in microns | Sample No.<br>in Fig. 1 | U ppm | Pb total<br>ppm | Ages in m.y.                              |   |   |  |  |   |      |
|---------------------------------------|-------------------------|-------|-----------------|---|---|---|--|--|---|------|
|                                       |                         |       |                 | $\frac{^{206}\text{Pb}}{^{204}\text{Pb}}$ | $\frac{^{207}\text{Pb}}{^{204}\text{Pb}}$ | $\frac{^{208}\text{Pb}}{^{204}\text{Pb}}$ | $\frac{^{206}\text{Pb}}{^{238}\text{U}}$ | $\frac{^{207}\text{Pb}}{^{235}\text{U}}$ | $\frac{^{207}\text{Pb}}{^{206}\text{Pb}}$ |      |
| LEB 2                                 | 9                       |       |                 |   |   |   |  |  |   |      |
| > 100, n.m.                           |                         | 648   | 51.3            | 611.1                                     | 58.48                                     | 82.08                                     | 451                                      | 554                                      | 1000                                      | + 14 |
| < 100 > 75, n.m.                      |                         | 711   | 52.1            | 614.3                                     | 55.34                                     | 78.93                                     | 423                                      | 493                                      | 833                                       | + 13 |
| < 75 > 53, n.m.                       |                         | 730   | 51.1            | 519.9                                     | 47.52                                     | 68.84                                     | 400                                      | 454                                      | 736                                       | + 21 |
| < 75 > 53, m.                         |                         | 960   | 55.9            | 460.7                                     | 41.52                                     | 66.13                                     | 330                                      | 361                                      | 560                                       | + 24 |
| < 42, m.                              |                         | 1018  | 59.8            | 421.16                                    | 38.70                                     | 59.01                                     | 332                                      | 356                                      | 515                                       | + 28 |
| BRA 1                                 | 10                      |       |                 |   |   |   |  |  |   |      |
| > 100, n.m.                           |                         | 418   | 26.08           | 1705                                      | 114.36                                    | 186.9                                     | 382                                      | 404                                      | 552                                       | + 11 |
| < 53 > 42, n.m.                       |                         | 442   | 26.87           | 1040                                      | 73.64                                     | 144.0                                     | 360                                      | 377                                      | 488                                       | + 11 |
| < 42, m.                              |                         | 496   | 29.29           | 814.7                                     | 60.50                                     | 126.7                                     | 342                                      | 359                                      | 472                                       | + 15 |
| BRA 2                                 | 10                      |       |                 |   |   |   |  |  |   |      |
| < 100 > 75, n.m.                      |                         | 530   | 34.4            | 715.8                                     | 56.15                                     | 74.88                                     | 388                                      | 411                                      | 540                                       | + 14 |
| < 75 > 53, m.                         |                         | 594   | 35.2            | 564.7                                     | 46.59                                     | 64.56                                     | 348                                      | 367                                      | 488                                       | + 30 |
| < 53 > 42, m.                         |                         | 666   | 39.1            | 467.0                                     | 40.98                                     | 59.39                                     | 339                                      | 358                                      | 483                                       | + 21 |
| < 42, m.                              |                         | 734   | 41.6            | 414.3                                     | 38.05                                     | 56.83                                     | 321                                      | 343                                      | 489                                       | + 25 |
| MATO 1                                | 11                      |       |                 |   |   |   |  |  |   |      |
| > 150                                 |                         | 415   | 25.6            | 246.1                                     | 27.63                                     | 59.80                                     | 309                                      | 312                                      | 338                                       | + 53 |
| < 150 > 75, n.m.                      |                         | 458   | 25.1            | 484.5                                     | 40.16                                     | 85.89                                     | 306                                      | 310                                      | 323                                       | + 31 |
| < 53 > 42, n.m.                       |                         | 669   | 32.1            | 1496                                      | 93.35                                     | 203.7                                     | 290                                      | 294                                      | 317                                       | + 12 |
| < 53, m.                              |                         | 789   | 37.6            | 887.2                                     | 60.92                                     | 140.1                                     | 279                                      | 282                                      | 297                                       | + 17 |
| MATO 2                                | 12                      |       |                 |   |   |   |  |  |   |      |
| > 75, n.m.                            |                         | 500   | 55.1            | 2757                                      | 253.0                                     | 360.9                                     | 638                                      | 820                                      | 1349                                      | + 4  |
| < 53 > 42, n.m.                       |                         | 641   | 59.1            | 6000                                      | 493.4                                     | 680.5                                     | 552                                      | 696                                      | 1195                                      | + 3  |
| < 53 > 42, m.                         |                         | 785   | 66.7            | 3876                                      | 306.4                                     | 461.5                                     | 508                                      | 614                                      | 1079                                      | + 4  |
| < 42, m.                              |                         | 882   | 67.7            | 3369                                      | 261.9                                     | 388.6                                     | 463                                      | 570                                      | 1129                                      | + 3  |
| RUSCADA                               | 14                      |       |                 |   |   |   |  |  |   |      |
| < 100 > 75, n.m.                      |                         | 2547  | 96.9            | 883.8                                     | 64.20                                     | 57.89                                     | 241                                      | 262                                      | 463                                       | + 31 |
| < 75 > 53, n.m.                       |                         | 2697  | 99.0            | 858.0                                     | 62.04                                     | 55.43                                     | 232                                      | 251                                      | 437                                       | + 14 |
| < 42                                  |                         | 3316  | 107.0           | 2054                                      | 125.5                                     | 77.74                                     | 215                                      | 229                                      | 372                                       | + 7  |
| COCCO 1                               | 15                      |       |                 |   |   |   |  |  |   |      |
| > 125, n.m.                           |                         | 615   | 27.9            | 2740                                      | 159.00                                    | 253.3                                     | 287                                      | 291                                      | 317                                       | + 9  |
| > 75 < 53, n.m.                       |                         | 753   | 32.2            | 8543                                      | 466.3                                     | 778.7                                     | 273                                      | 278                                      | 323                                       | + 4  |
| > 75 < 53, m.                         |                         | 870   | 37.5            | 2122                                      | 126.34                                    | 257.4                                     | 266                                      | 271                                      | 316                                       | + 9  |
| < 53, m.                              |                         | 1036  | 43.3            | 4036                                      | 226.7                                     | 470.1                                     | 260                                      | 266                                      | 310                                       | + 6  |
| GIUM 2                                | 17                      |       |                 |   |   |   |  |  |   |      |
| > 90, n.m.                            |                         | 2606  | 100.1           | 5792                                      | 335.4                                     | 183.3                                     | 258                                      | 276                                      | 429                                       | + 3  |
| < 75 > 53, n.m.                       |                         | 2538  | 97.1            | 12484                                     | 701.6                                     | 342.4                                     | 259                                      | 275                                      | 414                                       | + 12 |
| < 53 > 42, m.                         |                         | 3755  | 128.2           | 2194                                      | 139.19                                    | 131.1                                     | 227                                      | 236                                      | 336                                       | + 9  |
| < 42, m.                              |                         | 4034  | 129.4           | 15130                                     | 812.6                                     | 388.6                                     | 219                                      | 227                                      | 318                                       | + 2  |

Common Pb correction:  $^{206}\text{Pb}/^{204}\text{Pb} = 18.3$ ;  $^{207}\text{Pb}/^{204}\text{Pb} = 15.5$



Table 3 Analytical data of monazite samples

| SAMPLE<br>size fraction<br>in microns | Sample No.<br>in Fig. 1 | U ppm | Pb total<br>ppm | Ages in m.y.                              |   |   |  |  |   |         |
|---------------------------------------|-------------------------|-------|-----------------|---|---|---|--|--|---|---------|
|                                       |                         |       |                 | $\frac{206_{\text{Pb}}}{204_{\text{Pb}}}$ | $\frac{207_{\text{Pb}}}{204_{\text{Pb}}}$ | $\frac{208_{\text{Pb}}}{204_{\text{Pb}}}$ | $\frac{206_{\text{Pb}}}{238_{\text{U}}}$ | $\frac{207_{\text{Pb}}}{235_{\text{U}}}$ | $\frac{207_{\text{Pb}}}{206_{\text{Pb}}}$ |         |
| FUSIO                                 | 13                      | 6577  | 55.4            | 476.7                                     | 36.70                                     | 792.5                                     | 22.0                                     | 21.9                                     | 11 + 31                                   |         |
| RUSCADA                               | 14                      | 4605  | 61.6            | 436                                       | 34.92                                     | 1397                                      | 22.3                                     | 22.3                                     | 24 ± 41                                   |         |
| COCCO 1 > 100                         | 15                      | 4107  | 530             | 6971                                      | 375.8                                     | 18700                                     | 252                                      | 255                                      | 277 ± 4                                   |         |
| COCCO 1 < 100                         | 15                      | 4467  | 500             | 5884                                      | 320.2                                     | 17160                                     | 206                                      | 213                                      | 283 ± 4                                   |         |
| SOME0                                 | 16                      | 12520 | 48.3            | 860.3                                     | 54.72                                     | 178.2                                     | 22.1                                     | 22.2                                     | 28 ± 16                                   |         |
| GIUM 1 > 53                           | 17                      | 10379 | 661             | 8284                                      | 447.2                                     | 8448                                      | 219                                      | 231                                      | 294 ± 3                                   |         |
| GIUM 1 < 53                           | 17                      | 8214  | 514             | 6626                                      | 360.7                                     | 7873                                      | 204                                      | 212                                      | 295 ± 3                                   |         |
| GIUM 2 > 100                          | 17                      | 9044  | 667             | 11637                                     | 617.2                                     | 12320                                     | 255                                      | 257                                      | 275 ± 3                                   |         |
| GIUM 2 < 53                           | 17                      | 9392  | 699             | 7412                                      | 699.0                                     | 8910                                      | 241                                      | 244                                      | 277 ± 2                                   |         |
| BRI 2                                 | 20                      | 7156  | 61.9            | 662.2                                     | 45.61                                     | 1122                                      | 22.7                                     | 22.8                                     | 37 ± 21                                   |         |
| BRI 4                                 | 90                      | 21    | 6549            | 50.5                                      | 1081                                      | 64.87                                     | 1777                                     | 20.9                                     | 20.8                                      | 21 ± 10 |

Common Pb correction:  $\frac{206_{\text{Pb}}}{204_{\text{Pb}}} = 18.5$ ;  $\frac{207_{\text{Pb}}}{204_{\text{Pb}}} = 15.5$

1975; HÄNNY et al., 1975). The age patterns of fig. 2 allow to distinguish three zircon groups:

- Group 1 forms a comparatively narrow band which intercepts the concordia curve at 280 to 340 m.y. and which extends parallel to the curve indicating thereby a lead loss less than 100 m.y. ago.
- Group 2 occupies an area that can be delineated by the 150, 470 and 750 m.y. time marks on the concordia curve. The data points of psammitic to psephtitic gneisses (BRA 1, BRA 2) also plot in this field.
- The zircons of group 3 exhibit slightly curved arrays with an approximate upper intercept at 2000 m.y. and a lower intercept at about 300 m.y. Both samples were collected from metasediments.

By redrawing fig. 2 using a different scale, group 1 and 2 are more readily distinguishable (fig. 3). Group 1 may now be defined by those zircon populations which exhibit an array with a lower intercept of less than 100 m.y. and an upper intercept of about 300 m.y. The data points are contained in the upper part of a wedge shaped area shown in fig. 3 and defined by the following time marks: 20, 80, 280 and 320 m.y. Most of the zircons of the second group yield arrays with lower intercepts of 150 to 250 m.y. (fig. 3) and 400-450 m.y. (fig. 2, samples BES and SIM).

These two zircon groups exhibit a systematic regional distribution. Group 1 occupies an area between the Antigorio valley and the Simplon pass area, whereas Group 2 occurs to the East of the Antigorio valley and to the North of the Simplon pass. Only the samples EIS and TEG do not fit the regional distribution pattern.

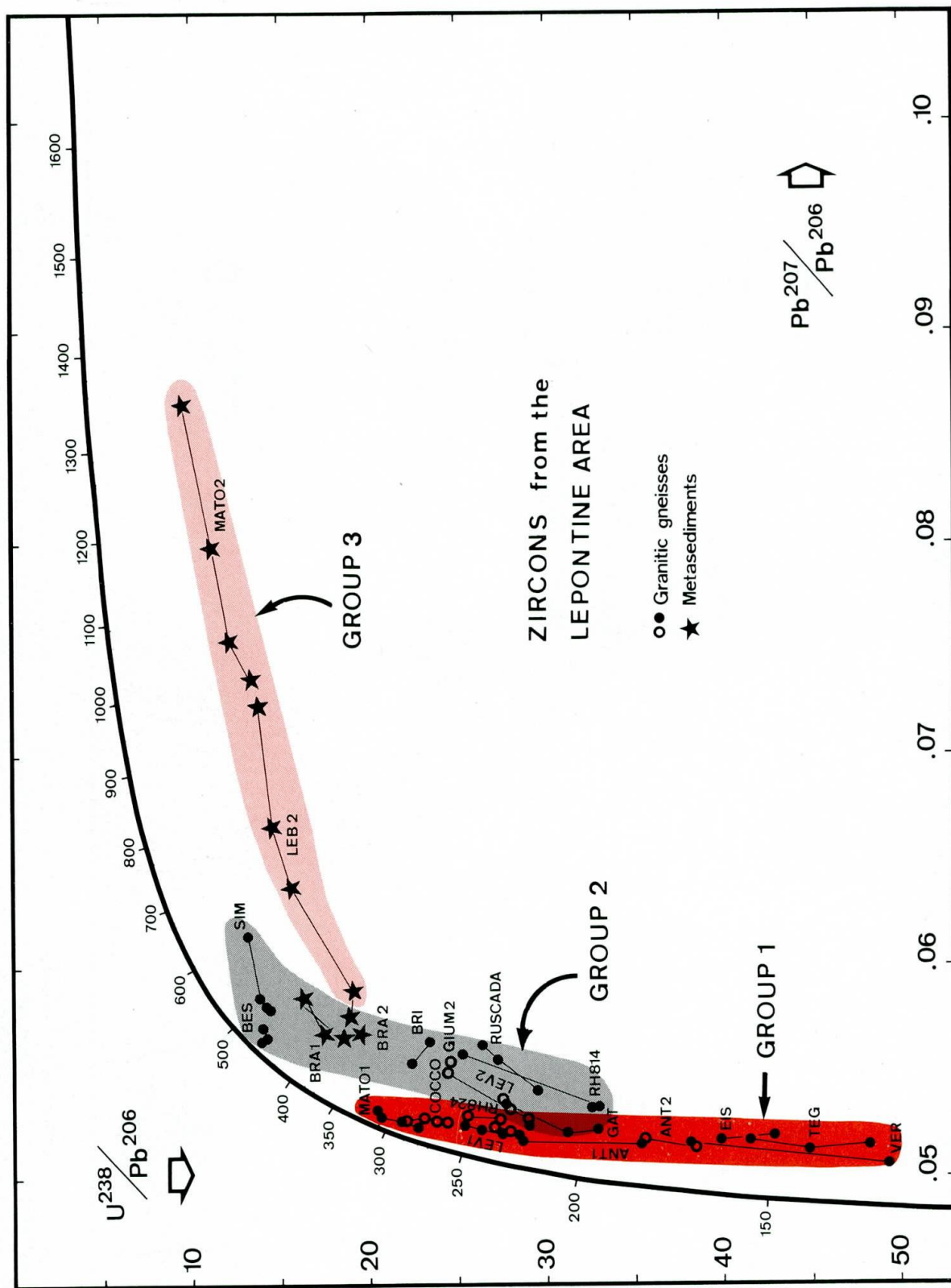


Fig. 2 Zircon data points from the Lepontine area. Sample locations are shown in fig. 1. Data points connected with tie-lines denote different size fractions and/or with differing magnetic susceptibilities of a zircon population separated from one rock sample.

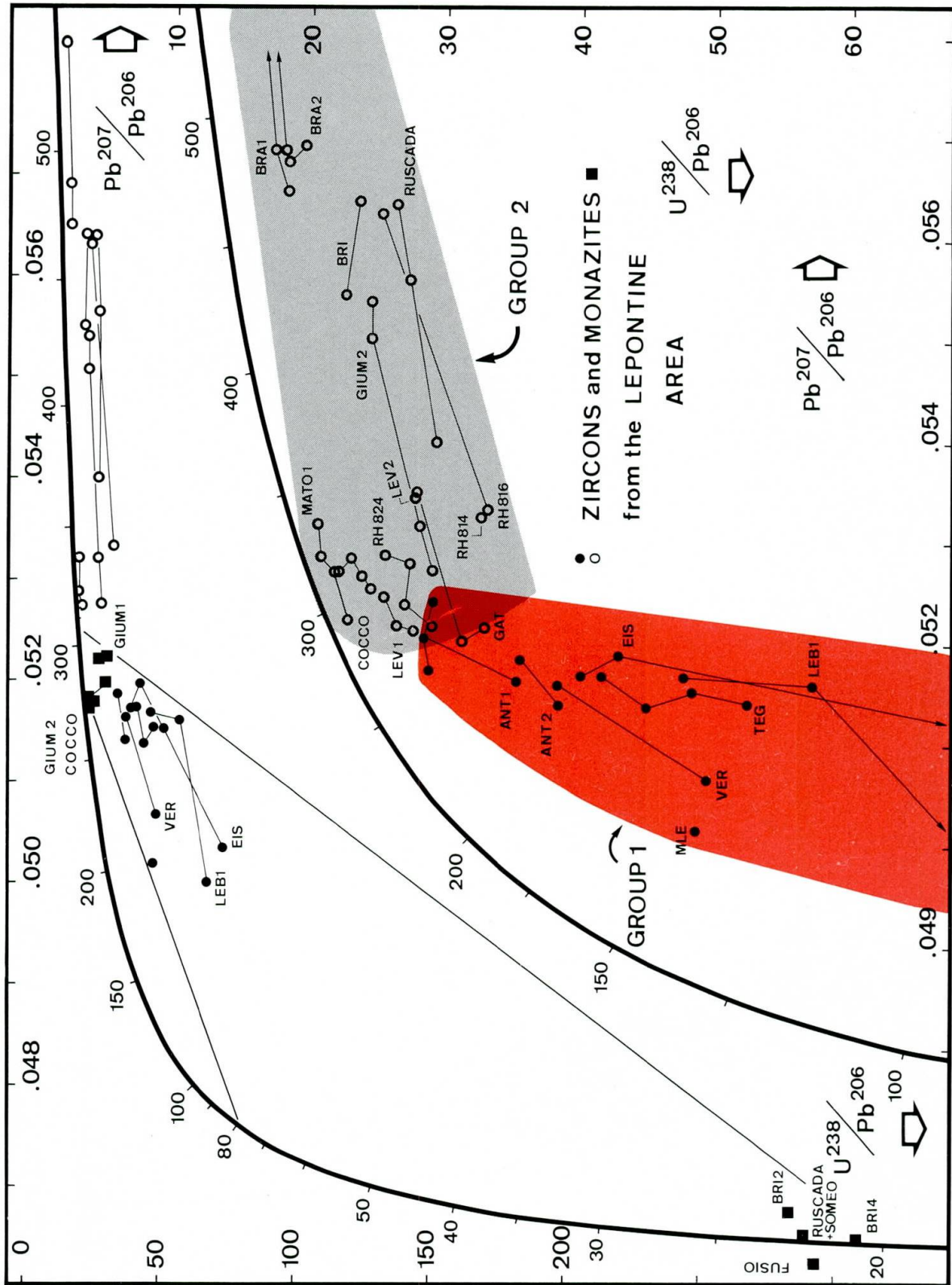


Fig. 3 Zircon (circles) and monazites (squares) data points from the Lepontine area. Open circles denote samples with lower intercept ages of about 150 to 250 m.y. (group 2) and full circles of 20 to 80 m.y. (group 1). Different zircon fractions of a suite from one rock sample are connected by tie-lines. The data points of all zircon suites, except BRA 2, shown in this figure exhibit linear arrays within analytical uncertainties. These uncertainties are discussed in the section «Results» and the error of the  $^{207}\text{Pb}/^{206}\text{Pb}$  ages are listed in tables 2 and 3.

It is evident that the U-Pb system of these two groups was disturbed at different times to different degrees. The U-Pb system of the zircons of group 1 was more severely disturbed during the Alpine metamorphism than those of group 2. Two points should be stressed:

- The degree of the disturbance is inversely related to the degree of the main Alpine thermal metamorphism. The thermal metamorphism reached a higher grade in the area to the East of the Antigorio valley than to the West.
- The degree of the disturbance does not correlate with the uranium concentrations of the zircon populations (table 2).

### Discussion

The interpretation of the zircon data from the Lepontine area relies on the interpretation of zircon ages from areas outside the influence of the Alpine metamorphism. Fig. 4 shows in a schematic fashion the U-Pb age patterns of zircons and monazites from areas where there is either no mineralogical evidence for an Alpine metamorphism (Southern Alps, Silvretta) or else the Alpine thermal metamorphism only reached greenschist facies conditions (Gotthard massive, Bernina (?)). Two cases should be distinguished:

- In areas where the Caledonian event dominated, detrital zircons from paragneisses point to average minimum crystallization ages of 1600 to 2500 m.y. and to a major lead loss 400 to 500 m.y. ago. Zircons from granitic gneisses cluster close to the concordia curve between 400 and 450 m.y. Concordant monazite ages from the Southern Alps of 450 m.y. testify for the existence of a Caledonian event. Rb-Sr whole rock data also support the existence of this event (GRAUERT and ARNOLD, 1968). ALLÈGRE et al. (1974), however, pointed out that the zircon age pattern could also be interpreted as indicating a Cadomian event 550 m.y. ago. Partial lead loss 300 m.y. ago would produce then the observed age pattern. So far, however, no independent evidence has been found for a Cadomian event in these areas.
- In areas where the Hercynian event dominated as in the Ivrea zone, zircon age patterns point to a strong Pb loss 280-300 m.y. ago. Concordant monazite ages of 270 to 320 m.y. also point to a high grade Hercynian event (KÖPPEL, 1974; KÖPPEL and GRÜNENFELDER, in preparation).
- Similar age patterns have been reported from other parts of Central Europe (e.g. GEBAUER and GRÜNENFELDER, 1973; GRAUERT et al., 1973, 1974; GEBAUER, 1975; SCHENK, 1980).

Not recrystallized zircons with high trace element concentrations, e.g. U > 2000 ppm, from postmetamorphic intrusive rocks normally yield discordant age patterns demonstrating a continuous or recent Pb loss possibly due to uplift, e.g. Orfano granite, gneiss chiari (KÖPPEL and GRÜNENFELDER, 1971).

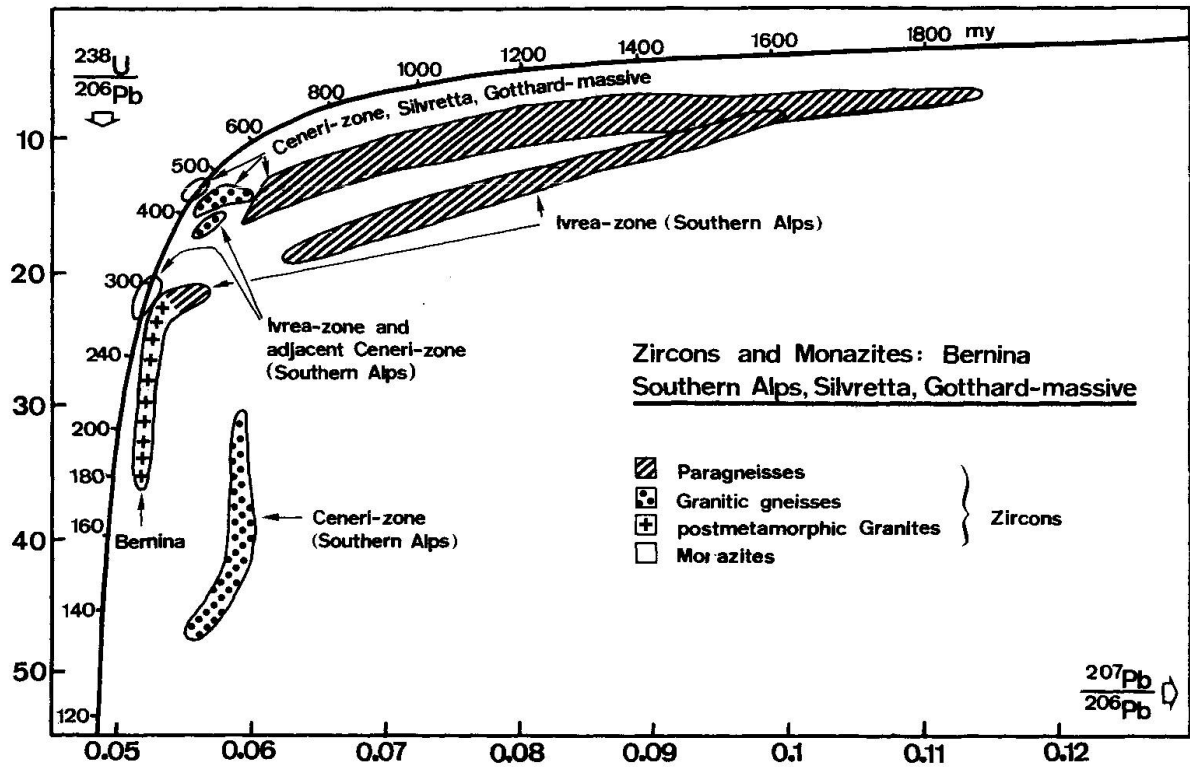


Fig. 4 Summary of zircon and monazite data from areas not affected by the mid-Tertiary thermal metamorphism. Data from GRAUERT and ARNOLD (1968), HÄNNY et al. (1975), KÖPPEL and GRÜNENFELDER (1971), KÖPPEL (1974) and NUNES and STEIGER (1974).

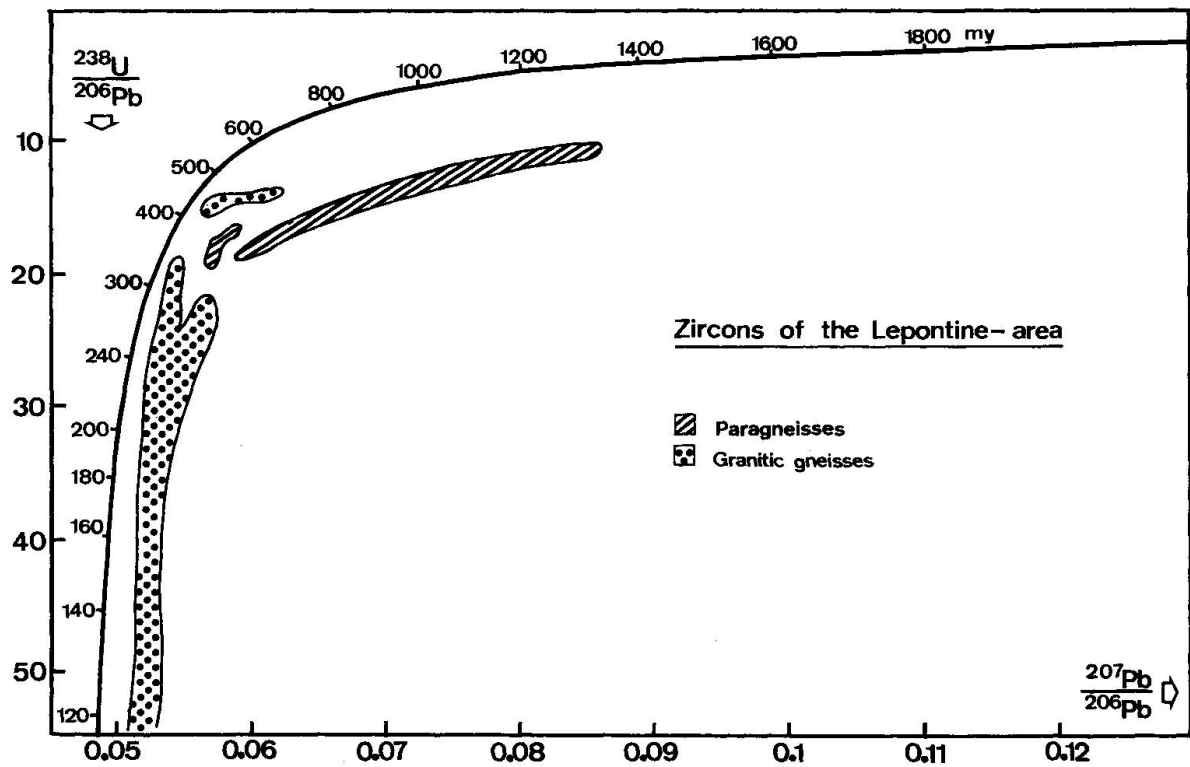


Fig. 5 Summary of zircon data from the Lepontine area where the mid-Tertiary thermal metamorphism reached amphibolite facies conditions. The data field of granitic gneisses extends to apparent  $^{238}\text{U}/^{206}\text{Pb}$  ages of 80 m. y.

It should be noted that zircons from granitic rocks frequently contain an inherited old lead component which probably is located in old often rounded cores of euhedral zircon crystals or is present in inherited crystals which still retain a rounded habit. Such zircon populations yield age patterns pointing in the direction of zircon data points from metasediments. The protolith of such granitic rocks was therefore either a sediment or the magma was contaminated with sedimentary material.

From these results it is obvious that the U-Pb system in zircons is on the one hand extremely resistant to a *complete* resetting during metamorphism, but on the other hand the same system may be *partially* opened by mild events. Thus precise and geologically significant ages can only be obtained from concordant or near-concordant ages. Discordant age patterns yield significant ages only if the zircon population is free of inherited zircon crystals and provided their U-Pb system was opened only once after crystallization, for example in response to a metamorphic event. The zircon ages, however, offer the unique opportunity to see through periods of metamorphism and thereby allow a reasonable reconstruction of the history of young, polymetamorphic areas.

The most striking feature is the close resemblance of the data pattern of the zircons from the Lepontine area (fig. 5) with that of zircons from regions much less or not at all influenced by the Alpine metamorphism (fig. 4). Except for the zircon data from the Tertiary intrusion in the Bergell area (GULSON and KROGH, 1973) and from a pegmatite near Gorduno (KÖPPEL and GRÜNENFELDER, in prep.) the zircon age pattern neither points to the existence of Alpine intrusions nor does it necessarily reflect the existence of the Alpine event that reached amphibolite facies conditions. The pattern may be interpreted as indicating Caledonian and Hercynian events including more recent lead losses possibly due to uplift; some of the data points may also be explained by a continuous lead loss. As there can be no doubt about the existence of a strong thermal metamorphism during the Alpine orogeny, this age pattern is striking evidence that the behaviour of the U-Pb system in zircons does not faithfully record each successive event but strongly depends on the thermal history of the zircons themselves and on their crystal-chemical state (SOMMERAUER, 1976).

During a first metamorphic event the crystal lattice recrystallized increasing thereby the resistivity of the U-Pb system to Pb losses during the following thermal events. Because the thermal events followed each other in rapid succession, radiation damage could not sufficiently damage the zircon lattice and thus the Alpine event was not as successful in opening the U-Pb systems as were earlier periods of metamorphism. Therefore the zircon age pattern still reflects the pre-Alpine history of the rocks which obviously was similar to that observed for example in the Southern Alps and elsewhere.

## CALEDONIAN GRANITIC GNEISSES

On the basis of the results gathered from areas outside the Alpine metamorphism one has to conclude from the zircon data that the Simano augengneiss (SIM) and the Berisal gneiss (BES) are Caledonian in age. The zircons formed a closed system for uranium and lead since the time of their formation or severe resetting 450 m.y. ago. Their age pattern as well as their morphology show that they are a mixed population consisting of longprismatic euhedral zircons and of recrystallized zircons with a rounded habit, indicating therefore an anatectic origin, or possibly assimilation of sedimentary material.

## HERCYNIAN GRANITIC GNEISSES

On the basis of their upper intercept ages of < 340 m.y, the following samples are interpreted as representing rocks of Hercynian ages (fig. 3): Cocco, Matorello (MATO 1), Leventina (LEV 1, 2), Verampio (VER), Antigorio (ANT 1, 2), Eisten (EIS), Tegna (TEG) and from the Bodengo area RH 824. The age pattern of most of their zircon suites indicates that they contain only small amounts (MATO 1, COCCO, LEV 2, RH 824) or possibly no inherited zircons (ANT, EIS, LEV 1, TEG, LEV 1, VER). The latter samples belong to the group with lower intercept ages of < 100 m.y. occurring mainly in the Simplon-Antigorio area. It thus appears that these granites are of a different origin (I-type granites <?>) than those of the eastern area where inherited zircons are common indicating the presence of S-type (?) granites.

There are several samples with age patterns that cannot be interpreted unambiguously as indicating Hercynian or Caledonian ages for the rocks. The samples from Brione (BRI), Giumaglio (GIUM), Ruscada and Bodengo (RH 814, 816) may either represent Caledonian zircon populations with some inherited zircons or else they may represent Hercynian populations with comparatively higher proportions of inherited zircons. The following samples deserve further considerations:

*Cocco:* The zircons from the Cocco granite-gneiss yielded an age pattern that points to an Hercynian age of the rock. The upper intercept age of 330 to 350 m.y. is high compared to the upper intercept age of 270 to 285 m.y. of the monazite. We interpret the monazite age to be the time of crystallization; the zircon age pattern then points to the presence of inherited zircons and therefore to an anatectic origin of the Cocco granite-gneiss.

Furthermore, the similar petrography, the similar zircon age patterns and uranium concentrations of the Cocco- and Matorello-gneisses underline their

petrographic cogeneity. The results comport with the conclusion that these granitic bodies predate the main thermal metamorphism of the Alpine orogeny (TROMMSDORFF, 1966).

*Ruscada*: The Ruscada gneiss intrudes the Cocco gneiss and therefore the zircon age pattern with an upper intercept age of 900 to 1100 m. y. demonstrates a significant inherited zircon component.

The concordant monazite age of 22.5 m. y. agrees with the monazite age pattern observed in the Lepontine area which indicates that the end of prograde conditions occurred about 20 to 25 m. y. ago in the central part of the Lepontine area (KÖPPEL and GRÜNENFELDER, 1975, 1978).

*Giunaglio*: The zircons from the aplitic gneiss (GIUM 2) have high uranium concentrations similar to those from the Ruscada gneiss. Their age patterns are also similar. However, their upper intercept age of 650 to 700 m. y. is lower than that of the Ruscada gneiss (900 to 1100 m. y.). Both rocks are possibly part of the same unit of late Hercynian granitic to aplitic intrusives with differing amounts of inherited zircons. The upper intercept age of the monazites indicates an age of 270 to 280 m. y. which is indistinguishable from that of the Cocco gneiss (270 to 285 m. y.), and we interpret this age as the time of the granitic intrusions.

The monazites from the paragneiss phase of the migmatite complex (GIUM 1) yielded a distinctly higher upper intercept age, depending on the time of lead loss during the Alpine metamorphism, of 285 to 305 m. y. than the monazites from the granitic gneisses. This higher age possibly indicates a period of regional metamorphism.

#### DISCUSSION OF THE LOWER INTERCEPT AGES OF THE ZIRCONS

The significance of the lower intercept ages of 150 to 250 m. y. is not evident. Two possibilities should be considered:

- The presence of inherited and newly formed zircons in Caledonian or Hercynian granitic gneisses coupled with a comparatively small lead loss during the Alpine metamorphism 20 to 30 m. y. ago would produce relatively high lower intercept ages.
- One may, on the other hand, be tempted to compare the intercepts of 200 to 250 m. y. with the late Hercynian event observed elsewhere in the Alps, for example in the Monte Rosa granite gneiss (HUNZIKER, 1970,  $260 \pm 10$  m. y., Rb-Sr whole rock measurements) and surrounding rocks (KÖPPEL and GRÜNENFELDER, 1975,  $260 \pm 5$  m. y., U-Pb measurements of monazites), or in the western part of the Hohe Tauern (SATIR, 1975,  $226 \pm 26$  m. y., Rb-Sr whole



rock measurements). The intercept ages towards 150 m.y. could then be the result of a further lead loss during the Tertiary Alpine metamorphism.

The zircons with lower intercept ages of 20 to 80 m.y. reflect the Alpine events of a high pressure metamorphism followed by a thermal metamorphism. Thus it seems likely that the regional distribution of the two zircon groups with differing lower intercept ages has a geological significance reflecting different histories. One may speculate that the zircons with the intercept ages in the range of 150 to 250 m.y. were annealed during a late Hercynian event to such a degree that their U-Pb systems hardly registered the Alpine event, whereas this annealing mechanism was not operative in the rocks to the East of Antigorio valley and to the North of the Simplon pass because either these rocks were not subjected to a late Hercynian event or else these granitic rocks postdate this event.

#### ZIRCONS FROM PARAGNEISSES

The zircon age pattern from the paragneiss MATO 2 resembles that of paragneisses observed in the Southern Alps, in the crystalline rocks of the Silvretta nappe and of the Gotthard massive. Where these metasediments are intruded by granitic gneisses containing zircons yielding a Caledonian crystallization age, this age is also a minimum age for the sedimentation of the paragneisses. Rb-Sr systematics indicate that the sediments were deposited in late pre-Cambrian to Cambrian time (GRAUERT, 1969). The existence of Silurian to Carboniferous sediments in the Eastern Alps suggests the possibility that metasediments of similar depositional age might also be present in the central part of the Alps where all stratigraphic records of pre-Upper Carboniferous sediments have been obliterated by metamorphism. Therefore the existence of upper Silurian or younger Palaeozoic sediments in this part of the Alps can only be demonstrated if metasediments are found containing detrital zircons which still retain a Caledonian age pattern. The presence of pre-Mesozoic metaconglomerates in the Lebedun and the Maggia nappes (WENK and GÜNTHERT, 1960) containing pebbles of granitic gneisses offered the opportunity of further elucidating the problem of sedimentation ages of the pre-Mesozoic metasediments.

Four zircon suites from metasediments were analyzed: MATO 2, a metasediment from the Maggia nappe, LEB 2 and BRA 2, two augengneiss pebbles from the Lebedun nappe, resp. Maggia nappe, and BRA 1, the matrix of sample BRA 2. Whereas the sedimentary nature of the Lebedun conglomerate is not disputed, the nature of the conglomerate gneiss in the area of the P. di Braga is, according to M. Huber (personal communication) open to discussion. According to recent structural investigations by M. Huber, the metaconglomerates may be the product of intensive shearing along the contact between Mesozoic



Fig. 6 Deformed pebbles of the metaconglomerate NE of Poncione di Braga in a matrix of augengneiss and biotite schist.

sediments and pre-Mesozoic crystalline rocks and then would be of tectonic origin. The original nature was, however, obscured by three subsequent phases of deformation. GÜNTHER (1954) (fig. 6) described a variety of strongly deformed components occurring in the metaconglomerate such as different types of quartzites, hornblende-gneisses, aplitic gneisses, gneisses and schists and thereby argued for a sedimentary origin of the conglomerate. WENK and GÜNTHER (1960) discussed the metapsephites of the Lebendun series and the Maggia nappe as well as of the Mesozoic Bündnerschiefer, where probably tectonically embedded gneiss fragments occur. No conclusive evidence for the tectonic origin of the conglomerates at the sample locality can be found. The authors favour at the present a sedimentary origin of this rock.

The zircon age pattern of the samples BRA 1 and BRA 2 are identical and differ markedly from that of sample MATO 2 (fig. 2). The three coarser zircon fractions of sample LEB 2 follow the pattern of sample MATO 2 whereas the two finer fractions plot close to the data points of BRA 1 and 2. This pattern is not only due to different degrees of lead loss but is related also to the appearance of idiomorphic, long prismatic crystals: more than 90% of the zircons in sample MATO 2 are well rounded but already in the coarser fractions of the sample LEB 2 idiomorphic zircons and well rounded crystals coexist in propor-

tions of about 4:5 which then changes to 5:3 in the finer fractions; in the sample BRA 1 and 2 idiomorphic zircons strongly dominate.

The age patterns of samples BRA 1, 2 and the finer fractions of LEB 2 are in our opinion best explained by assuming that the zircons suffered a drastic resetting of their U-Pb systems about 450 m.y. ago by a severe lead loss and the formation of new zircons during a metamorphic event that lead to a partial melting of sedimentary material. Their present position below the data field defined by the samples BES and SIM is explained by further lead loss during Hercynian and/or Alpine events. The occurrence of these zircons in the matrix and in augengneiss boulders of a metaconglomerate demonstrates that the Caledonian source rocks were exposed to erosion and their detritus formed the psammitic and psephitic sediments. The sediments were subsequently metamorphosed and, according to GÜNTHERT et al. (1976) transformed in places to granitic rocks which today form the Matorello gneiss. It contains predominantly idiomorphic long prismatic zircons. Crystals with a rounded habit constitute less than 10% of the population. According to the age pattern, the formation of the Matorello granite occurred 300 m.y. ago. The zircon data are hence compatible with the origin of the Matorello gneiss as deduced from field observations by GÜNTHERT (1954, 1976).

The results demonstrate that the deposition of the pre-Permian metasediments occurred during two distinct periods:

- One cycle of sedimentation occurred prior to the period of the Caledonian metamorphism, i.e. prior to about 450 m.y., and
- a second cycle occurred between the Caledonian and Hercynian magmatic/metamorphic events. The results therefore prove the existence of sediments in the Central Alps which were deposited between the upper Ordovician and lower Carboniferous and which correlate in time with the Grauwacken zone of the Eastern Alps. The Caledonian event was followed by a period of uplift, cooling and erosion, and it seems therefore likely that the Caledonian event was of an orogenic nature and not only a deep seated thermal event. BORSI et al. (1973) concluded from petrological and geochronological evidence from rocks of the Merano-Mules-Anterselva Complex south of the Tauern Window that the Caledonian event exhibits all characteristics of an orogeny. CLIFF (1980) also reported geochronological evidence for tectonic activity during the lower Palaeozoic period of magmatism in rocks of the Deferegger Mountains south of the Tauern Window.

Another hypothesis may consider the sedimentation age of the metapsammites and -psephites to be the same as that of the other paragneisses, i.e. Upper pre-Cambrian to Cambrian. The presence of a predominantly idiomorphic zircon population with an age pattern typical of Caledonian orthogneisses would then imply that these zircons crystallized in -situ during the Caledonian metam-

orphism and that these rocks were probably devoid of zircons prior to this event. This possibility seems rather unlikely in view of the rare cases where paragneisses were found to contain almost entirely new zircon populations developed during metamorphism without signs of at least a partial melting.

The age pattern of samples BRA 1, 2 and LEB 2 may also be interpreted as indicating a strong Hercynian resetting of Precambrian zircon populations coupled with new zircon growth. The present occurrence of these zircons in metasediments would then, however, argue for a Permian to Mesozoic age of these sediments which is quite unlikely in view of the significant differences of their metamorphic grade in comparison with that of the neighbouring Mesozoic Bündnerschiefer (WENK and GÜNTHERT, 1960).

### Conclusions

The most striking result is the close resemblance of the zircon data pattern of meta-igneous rocks and metasediments of the Lepontine area, where the Tertiary metamorphism reached amphibolite facies conditions, with those from areas not influenced by this metamorphism. Therefore, if periods of metamorphism followed in comparatively rapid succession, the zircon U-Pb system records mainly the first event, whereas the later ones are only partially or not at all recorded because of the increased stability of the recrystallized zircon lattice.

All the granitic gneisses within the Lepontine area to the West of Mera valley so far yielded zircon ages demonstrating either a Caledonian or Hercynian age. Only the zircons from Tertiary intrusives yield age patterns that demonstrate the existence of a young magmatic event.

Detrital zircons in metasediments or in conglomeratic components therein demonstrate the existence of two periods of sedimentation, a pre-Taconian one, i.e. Ordovician or older, and a second one between the periods of Caledonian and Hercynian metamorphism. The Caledonian event in the Central Alps was therefore of an orogenic nature.

The hypothesis that the Matorello gneiss derived from the neighbouring metasediments accords with the zircon systematics.

The regional distribution of the zircon age patterns indicates different origins of the granitic magmas rather than varying degrees of fortuitous assimilation of metasediments. Thus the lower intercept ages of 20–80 m.y. of the zircons from the Simplon-Antigorio area and the paucity or absence of noticeable inherited zircons possibly argues for I-type granites that were formed after the regional Hercynian metamorphism. The presence of inherited zircons in almost all of the granitic gneisses in the area between the Antigorio and Mera valleys indicates a S-type origin of these magmatic bodies. The absence of a marked

Pb-loss during the Alpine metamorphism is best explained by arguing that these granites predate the last Hercynian thermal event so that their zircons were annealed prior to the Alpine metamorphism and therefore were less susceptible to Pb-losses than those of the Simplon-Antigorio area.

High apparent ages of monazites from an area well within the region of amphibolite facies metamorphism during the Alpine metamorphism supports the view that the U-Pb system in monazites is resistant to resetting under elevated temperatures and that young concordant monazite ages within the Lepontine area reflect the end of prograde metamorphic conditions related to the Alpine orogeny.

#### Acknowledgements

We wish to thank Prof. A. Gansser for donating the augengneiss pebble from the Lebendun conglomerate. We also acknowledge the helpful discussions with Miss C. Simpson, Mr. M. Huber and Prof. A. Gansser, Mr. W. Wittwer was responsible for the mineral separation, and Mr. O. Krebs greatly assisted us with the chemical separation and the mass spectrometric analyses.

We thank Dr. D. Gebauer and Dr. F. Oberli for improving the manuscript by their helpful criticism.

#### Appendix: Sample localities and sample description

(sample No. refers to fig.1)

##### LEB 2 (No. 9)

Tunnel between Robiei and Val Bedretto. Augengneiss pebble in a metaconglomerate of the Lebendun-Series consisting of quartz, plagioclase, K-feldspar, biotite, muscovite, chlorite and some carbonate.

##### BRA 1 (No. 10)

NE of P. di Braga, Val di Peccia; 685.25 / 143.32.

Metapsammitic matrix (arkosic) of the conglomerate gneiss consisting of irregular granoblastic layers of quartz, K-feldspar, plagioclase, biotite and muscovite.

##### BRA 2 (No. 10)

Same locality as sample BRA 1. Deformed pebble of augengneiss. Quartz and K-feldspar or K-feldspar and plagioclase form granoblastic lenses. Biotite and muscovite in the schistose matrix.

##### MATO 1 (No. 11)

Western shore of Lake Sambucco. Composite sample from 692.45 / 146.775 to 692.70 / 146.500. Granodioritic, almost massive, coarse grained gneiss containing quartz, K-feldspar, plagioclase, porphyroblast of alkalifeldspar and biotite concentrated in nests. Minor constituents are clinozoisite-epidote.

**MATO 2 (No. 12)**

Eastern shore of Lake Sambucco, 693.85 / 146.15.

Granoblastic paragneiss consisting of quartz, plagioclase and biotite.

**FUSIO (No. 13)**

Road cut S of Fusio, 694.06 / 144.16.

Grano- to lepidoblastic paragneiss consisting of quartz, plagioclase, garnet, biotite and muscovite.

**RUSCADA (No. 14)**

Val di Prato, 695.45 / 138.55

Fine grained massive to slightly schistose, aplitic gneiss consisting of quartz, K-feldspar, plagioclase, muscovite and biotite. The Ruscada gneiss intrudes paragneisses and the Cocco gneiss causing lit-par-lit and nebulitic to magmatitic structures. It contains xenoliths of the country rock.

**COCCO (No. 15)**

Val Tomeo, E of Broglio, 695.85 / 136.90

The granodioritic, almost massive coarse grained gneiss consists of quartz, K-feldspar, plagioclase and biotite.

**SOMEO (No. 16)**

Road cut SE of Someo, 694.65 / 126.73

Grano- to lepidoblastic paragneiss with quartz, plagioclase, biotite and muscovite.

**GIUM 1 (No. 17)**

Road cut NW of Giumaglio, 695.20 / 125.95

Grano- to nidoblastic paragneiss consisting of quartz, K-feldspar, plagioclase, biotite and muscovite.

**GIUM 2 (No. 17)**

Same locality as GIUM 1

Light colored, massive, coarse grained granoblastic gneiss with quartz, K-feldspar, plagioclase, biotite and muscovite. This gneiss intrudes the paragneisses (GIUM 1) forming thereby a migmatite.

**BRI 1 (No. 19)**

Quarry Togni, NW of Brione, 703.75 / 128.25

Massive to schistose gneiss (Verzascagneiss) with quartz, plagioclase, K-feldspar, biotite and muscovite.

**BRI 2 (No. 20)**

Road cut N of Brione, 704.40 / 128.95

Granoblastic gneiss with quartz, plagioclase, biotite and muscovite.

**BRI 4 (No. 21)**

Road cut SW of Brione, 705.05 / 126.80

Granoblastic gneiss with quartz, plagioclase, hornblende, biotite and garnet.

## References

- ALLÈGRE, C.J., ALBARÈDE, F., GRÜNENFELDER, M. and KÖPPEL, V. (1974):  $^{238}\text{U}/^{206}\text{Pb}$  -  $^{235}\text{U}/^{207}\text{Pb}$  -  $^{232}\text{Th}/^{208}\text{Pb}$  zircon geochronology in alpine and non-alpine environment. *Contrib. Mineral. Petrol.* 43, 163-194.
- BORSI, S., DEL MORO, A., SASSI, F.P. and ZIRPOLI, G. (1973): Metamorphic evolution of the Austridic rocks to the south of the Tauern Window (Eastern Alps): radiometric and geopetrologic data. *Mem. Soc. Geol. Italiana*, 12, 549-571.
- CLIFF, R.A. (1980): U-Pb isotopic evidence from zircons for lower Palaeozoic tectonic activity in the Austroalpine nappe, the Eastern Alps. *Contrib. Mineral. Petrol.* 71, 283-288.
- CORFU, F. (1980): U-Pb and Rb-Sr systematics in a polyorogenic segment of the Precambrian shield, central southern Norway. *Lithos* 13, 305-323.
- EVANS, B.W. and TROMMSDORFF, V. (1978): Petrogenesis of the garnet lherzolite, Cima di Gagnone, Lepontine Alps. *Earth and Planet. Sc. Lett.* 40, 333-348.
- FREY, M., HUNZIKER, J.C., FRANK, U., BOQUET, J., DAL PIAZ, G.V., JÄGER, E. and NIGGLI, E. (1974): Alpine metamorphism of the Alps, a review. *Schweiz. Min. Petr. Mitt.* 54 2/3, 247-290.
- FREY, M., TROMMSDORFF, V. and WENK, E. (1980): Alpine metamorphism of the Central Alps. Excursion No. VI; Geology of Switzerland, a guide-book. Wepf & Co, Basel.
- GEBAUER, D. and GRÜNENFELDER, M. (1973): Vergleichende U/Pb- und Rb/Sr-Altersbestimmungen im bayerischen Teil des Moldanubikums. *Fortschr. Mineral.* 50, Beih. 34, 4.
- GEBAUER, D. (1975): Rb-Sr Gesamtgesteins- und Mineralsysteme sowie U-Pb Systeme in Zirkonen während der progressiven Gesteinsmetamorphose. Dissertation ETH Zürich.
- GEBAUER, D. and GRÜNENFELDER, M. (1979): U-Th-Pb dating of minerals, in «Lectures in Isotope Geology», ed. E. Jäger and J.C. Hunziker, Springer Verlag, pp. 105-131.
- GRAUERT, B. (1969): Die Entwicklungsgeschichte des Silvretta-Kristallins auf Grund radiometrischer Altersbestimmungen. Dissertation, München.
- GRAUERT, B. and ARNOLD, A. (1968): Deutung diskordanter Zirkonalter der Silvrettadecke und des Gotthardmassives. *Contrib. Mineral. Petrol.* 20, 34-56.
- GRAUERT, B., HÄNNY, R. and SOPTRAJANOVA, G. (1973): Age and origin of detrital zircons from the pre-Permian basements of the Bohemian massif and the Alps. *Contrib. Mineral. Petrol.* 40, 105-130.
- GRAUERT, B., HÄNNY, R. and SOPTRAJANOVA, G. (1974): Geochronology of a polymetamorphic and anatectic gneiss region: The Moldanubicum of the area Lam-Deggendorf, Eastern Bavaria, Germany. *Contrib. Mineral. Petrol.* 45, 37-63.
- GULSON, B.L. and KROGH, T.E. (1973): Old lead components in the young Bergell massif, south-east Swiss Alps. *Contrib. Mineral. Petrol.* 40, 239-252.
- GÜNTHER, A. (1954): Beiträge zur Petrographie und Geologie des Maggia-Lappens (NW Tessin). *Schweiz. Min. Petr. Mitt.* 34, 1-159.
- GÜNTHER, A., STERN, W.B. and SCHWANDER, H. (1976): Isochemische Granitgneisbildung im Maggia-Lappen (Lepontin der Zentralalpen). *Schweiz. Min. Petr. Mitt.* 56, 105-143.
- HÄNNY, R., GRAUERT, B. and SOPTRAJANOVA, G. (1975): Palaeozoic migmatites affected by high-grade Tertiary metamorphism in the Central Alps (Valle Bodengo, Italy). *Contrib. Mineral. Petrol.* 51, 173-196.
- HUBER, M.I. (1981): Geologisch-strukturelle Untersuchungen im oberen Maggiagebiet (Tessin, Schweiz). Diss. ETH Zürich.
- HUNZIKER, J.C. (1970): Polymetamorphism in the Monte Rosa, Western Alps. *Eclogae geol. Helv.* 63/1, 151-161.
- KÖPPEL, V. and GRÜNENFELDER, M. (1971): A study of inherited and newly formed zircons from paragneisses and granitised sediments of the Strona-Ceneri-Zone (Southern Alps). *Schweiz. Min. Petr. Mitt.* 51, 2/3, 385-409.

- KÖPPEL, V. (1974): Isotopic U-Pb ages of monazites and zircons from the crust-mantle transition and adjacent units of the Ivrea and Ceneri zones (Southern Alps, Italy). *Contrib. Mineral. Petrol.* 43, 55-70.
- KÖPPEL, V. and GRÜNENFELDER, M. (1975): Concordant U-Pb ages of monazite and xenotime from the Central Alps and the timing of the high temperature Alpine metamorphism, a preliminary report. *Schweiz. Min. Petr. Mitt.* 55/1, 129-132.
- KÖPPEL, V. and GRÜNENFELDER, M. (1978): The significance of monazite U-Pb ages; examples from the Lepontine area of the Swiss Alps. 4<sup>th</sup> Int. Conf. Geochronology, Cosmochronology and Isotope Geology, U.S. Geol. Survey Open-File Report 78-701, 226-227.
- KROGH, T. E. (1971): A simplified technique for the dissolution of zircons and the isolation of uranium and lead. Carnegie Institution, Annual Report, Geophysical Laboratory, pp. 341-344.
- LUDWIG, K. R. (1977): Effect of initial radioactive daughter disequilibrium on U-Pb isotope apparent ages of young minerals. *J. of Research U.S. Geol. Survey* 5, No. 6, 663-668.
- NUNES, P. D. and STEIGER, R. H. (1974): A U-Pb zircon and Rb-Sr and U-Th-Pb whole rock study of a polymetamorphic terrane in the Central Alps, Switzerland. *Contrib. Mineral. Petrol.* 47, 255-280.
- OVERSTREET, W. C. (1967): The geologic occurrence of monazite. U.S. Geol. Survey, prof. paper 530.
- SCHENK, V. (1980): U-Pb and Rb-Sr dates and their correlation with metamorphic events in the granulite-facies basement of the Serre, southern Calabria (Italy). *Contrib. Mineral. Petrol.* 73, 23-38.
- SATIR, M. (1975): Die Entwicklungsgeschichte der westlichen Hohen Tauern und der südlichen Oetztalmasse auf Grund radiometrischer Altersbestimmungen. *Mem. Ist. Geol. e Min. Università di Padova* XXX.
- SCHÄRER, U. (1980): U-Pb and Rb-Sr dating of a polymetamorphic nappe terrain: The Caledonian Jotun nappe, southern Norway. *Earth Planet. Sci. Lett.* 49, 205-218.
- SOMMERAUER, J. (1976): Die chemische Stabilität natürlicher Zirkone und ihr U-(Th)-Pb-system. Dissertation ETH Zürich, Nr. 5755.
- TROMMSDORFF, V. (1966): Progressive Metamorphose kieseliger Karbonatgesteine in den Zentralalpen zwischen Bernina und Simplon. *Schweiz. Min. Petr. Mitt.* 46/2, 431-460.
- WENK, E. (1969): Zur Regionalmetamorphose und Ultrametamorphose im Lepontin. *Fortschr. Mineralogie* 47, 34-51.
- WENK, E. and GÜNTHER, A. (1960): Über metamorphe Psephite der Lebendun-Serie und der Bündnerschiefer im NW-Tessin und Val d'Antigorio. Ein Diskussionsbeitrag. *Eclogae geol. Helv.* 53/1, 179-188.